

UNIVERSITY OF SOUTHAMPTON
SCHOOL OF ENGINEERING SCIENCES
AERODYNAMICS & FLIGHT MECHANICS GROUP

Viscous Instability of a Compressible Round Jet

by

Adriana M. Salgado and Neil D. Sandham

Report No. AFM-07/01

March 2007

COPYRIGHT NOTICE -

All right reserved. No parts of this publication may be reproduced, stored in a retrieval system, or transmitted, in any form or by any means, electronic, mechanical, photocopying, recording, or otherwise, without the permission of the Head of the School of Engineering Sciences, University of Southampton, Southampton SO17 1BJ, U.K.

© School of Engineering Sciences, University of Southampton

Viscous Instability of a Compressible Round Jet

Adriana M. Salgado and Neil D. Sandham

*Aerodynamics and Flight Mechanics Research Group
School of Engineering Sciences, University of Southampton
Southampton SO17 1BJ*

Abstract

The compressible linear stability equations are derived from the Navier Stokes equations in cylindrical polar coordinates. Numerical solutions for locally parallel flow are found using a direct matrix method. Discretization with compact finite difference is found to have better convergence properties than a Chebyshev spectral method for a round jet test case. The method is validated against previous results and convergence is tested for a range of jet profiles. Finally an e^n method is used to determine the dominant frequency of a Mach 0.9 jet.

1 Theory

1.1 Introduction

The aim of this report is to present a solution procedure for the compressible Orr-Sommerfeld equation. The starting point is the compressible Navier-Stokes Equations (NSE) which are written in a form that can be easily linearized and solved in order to find the eigenvalues and eigenvectors for spatial and temporal disturbances. This is done by firstly obtaining a polar version of the NSE; secondly, assuming that each of the variables (density - ρ , radial velocity - V_r , angular velocity - V_θ , streamwise velocity - V_z and temperature - T) can be separated into a mean, $\bar{\phi}$, and fluctuating value, ϕ' , where these fluctuations are modeled as: $\phi' = \hat{\phi}e^{i(\alpha z + n\theta - \omega t)}$; and thirdly, making assumptions about the behaviour of these mean and fluctuating quantities.

The end result is a linear system of the form: $L\hat{\phi} = \omega K\hat{\phi}$, where K and L are matrices and $\hat{\phi}$ is the array containing the values of the fluctuations at each radial (r) position away from the jet centre line. This is solved for various values of the wavenumber α (the temporal stability problem), or frequency ω (the spatial stability problem), at different z -locations along the jet axis.

The following sections detail each step of the derivation, including the numerical approach used to solve the system and obtain both the spatial and temporal disturbance structure.

1.2 Compressible Navier-Stokes Equations

In order to obtain the compressible Navier-Stokes Equations in polar coordinates we start from the non-conservative form of the compressible Navier-Stokes Equations in Cartesian coordinates, which are first given in dimensional form, using $*$ to denote a dimensional quantity. The equations for mass, momentum and energy conservation are:

$$\begin{aligned} \frac{\partial \rho^*}{\partial t^*} + u_j^* \frac{\partial \rho^*}{\partial x_j^*} + \rho^* \frac{\partial u_j^*}{\partial x_j^*} &= 0 \\ \rho^* \frac{\partial u_i^*}{\partial t^*} + \rho^* u_j^* \frac{\partial u_i^*}{\partial x_j^*} + \frac{\partial p^*}{\partial x_i^*} &= \frac{\partial \tau_{ij}^*}{\partial x_j^*} \\ \rho^* \frac{\partial e^*}{\partial t^*} + \rho^* u_i^* \frac{\partial e^*}{\partial x_i^*} + p^* \frac{\partial u_i^*}{\partial x_i^*} &= -\frac{\partial q_i^*}{\partial x_i^*} + \tau_{ij}^* \frac{\partial u_i^*}{\partial x_j^*} \end{aligned} \quad (1.1)$$

where the heat flux is given by, $q_i^* = -\kappa^* \frac{dT^*}{dx_i^*}$ and the viscous stress tensor is given by, $\tau_{ij}^* = \mu^* \left(\frac{\partial u_i^*}{\partial x_j^*} + \frac{\partial u_j^*}{\partial x_i^*} - \frac{2}{3} \frac{\partial u_k^*}{\partial x_k^*} \delta_{ij} \right)$.

The perfect gas law is given by:

$$p^* = \rho^* R^* T^* \quad (1.2)$$

constant specific heats are assumed so that energy is related to temperature by:

$$e^* = c_V^* T^* \quad (1.3)$$

with:

$$\gamma = \frac{c_P}{c_V}, R = c_P - c_V \text{ and } \frac{R}{c_V} = \gamma - 1.$$

Flow Characteristics

We define the Mach number as $M = u_R^*/\sqrt{\gamma R^* T_R^*}$, the Prandtl number as $Pr = c_P^* \mu_R^*/\kappa_R^*$ and the Reynolds number as $Re = \rho_R^* u_R^* L_R^*/\mu_R^*$. The subscript R refers to a reference value such as the reference velocity, u_R , corresponding to the jet core velocity, a reference length, L_R , corresponding to the radius of the jet, and other quantities corresponding to the behaviour of the flow at the exit from the jet nozzle. These reference values can be used to define our variables in a dimensionless form, such that: $x = x^*/L_R^*$, $u = u^*/u_R^*$, $T = T^*/T_R^*$, $t = t^* U_R^*/L_R^*$, $\kappa = \kappa^*/\kappa_R^*$, $\mu = \mu^*/\mu_R^*$ and $\rho = \rho^*/\rho_R^*$.

Sutherlands Law is used for viscosity and conductivity,

$$\mu = (T)^{\frac{3}{2}} \frac{(1+C)}{(T+C)} \quad (1.4)$$

$$\kappa = (T)^{\frac{3}{2}} \frac{(1+D)}{(T+D)} \quad (1.5)$$

Here T , μ and κ are already dimensionless and the constants, C and D , depend on the reference temperature in Sutherlands Law and the reference temperature for the jet, which are not necessarily the same. We used $C = 110.4/T_R$ with $T_R = 298.15K$. It is assumed here that $C = D$, and hence $\mu = \kappa$.

1.3 Dimensionless Navier-Stokes Equations

When we non-dimensionalize equations 1.1 and substitute in the previous relations for q_i , e and Sutherlands Law, we obtain the following form of the compressible Navier-Stokes:

$$\begin{aligned}
\frac{\partial \rho}{\partial t} + u_j \frac{\partial \rho}{\partial x_j} + \rho \frac{\partial u_j}{\partial x_j} &= 0 \\
\rho \frac{\partial u_i}{\partial t} + \rho u_j \frac{\partial u_i}{\partial x_j} + \frac{\rho}{\gamma M^2} \frac{\partial T}{\partial x_i} + \frac{T}{\gamma M^2} \frac{\partial \rho}{\partial x_i} &= \frac{1}{Re} \frac{\partial \tau_{ij}}{\partial x_j} \\
\rho \frac{\partial T}{\partial t} + \rho u_i \frac{\partial T}{\partial x_i} + (\gamma - 1) \rho T \frac{\partial u_i}{\partial x_i} &= \frac{\gamma}{Re Pr} \frac{\partial}{\partial x_i} \left(\kappa \frac{\partial T}{\partial x_i} \right) \\
&+ \frac{M^2 \gamma (\gamma - 1)}{Re} \tau_{ij} \frac{\partial u_i}{\partial x_j}
\end{aligned} \tag{1.6}$$

Now all the variables are dimensionless and can be written in vector form as follows.

Vector Form of Compressible Navier-Stokes Equations

$$\begin{aligned}
\frac{\partial \rho}{\partial t} + \underline{u} \cdot (\nabla \rho) + \rho (\nabla \cdot \underline{u}) &= 0 \\
\rho \frac{\partial \underline{u}}{\partial t} + \rho \underline{u} \cdot (\nabla \underline{u}) + \frac{1}{\gamma M^2} (\rho \nabla T + T \nabla \rho) &= \frac{1}{Re} \nabla \cdot \underline{\underline{\tau}} \\
\rho \frac{\partial T}{\partial t} + \rho \underline{u} \cdot (\nabla T) + (\gamma - 1) \rho T (\nabla \cdot \underline{u}) &= \frac{\gamma}{Re Pr} \nabla (\kappa (\nabla T)) + \frac{M^2 \gamma (\gamma - 1)}{Re} \underline{\underline{\tau}} \cdot (\nabla \underline{u})
\end{aligned} \tag{1.7}$$

Where $\underline{\underline{\tau}} = \mu (\nabla \underline{u} + \nabla \underline{u}^T - \frac{2}{3} \nabla \cdot \underline{u} \underline{I}) = \mu \underline{\underline{s}}$. The vector relations found in equation 1.7 and $\underline{\underline{s}}$, the stress tensor, are detailed in Appendix A.

1.4 Polar Form of the Compressible Navier Stokes Equations

The following are the complete compressible Navier Stokes Equations in cylindrical polar coordinates obtained by using the relations found in appendix A.

Polar Form of the Continuity Equation

$$\frac{\partial \rho}{\partial t} + \left(V_r \frac{\partial \rho}{\partial r} + \frac{V_\theta}{r} \frac{\partial \rho}{\partial \theta} + V_z \frac{\partial \rho}{\partial z} \right) + \rho \left(\frac{\partial V_r}{\partial r} + \frac{V_r}{r} + \frac{1}{r} \frac{\partial V_\theta}{\partial \theta} + \frac{\partial V_z}{\partial z} \right) = 0 \tag{1.8}$$

Polar Form of the r - Momentum Equation

$$\begin{aligned}
& \rho \frac{\partial V_r}{\partial t} + \rho \left(V_r \frac{\partial V_r}{\partial r} + \frac{V_\theta}{r} \frac{\partial V_r}{\partial \theta} - \frac{V_\theta^2}{r} + V_z \frac{\partial V_r}{\partial z} \right) + \frac{1}{\gamma M^2} \left(\rho \frac{\partial T}{\partial r} + T \frac{\partial \rho}{\partial r} \right) \\
&= \frac{1}{Re} \left[\mu \left(\frac{4}{3} \frac{\partial^2 V_r}{\partial r^2} + \frac{4}{3} \frac{1}{r} \frac{\partial V_r}{\partial r} + \frac{1}{3} \frac{1}{r} \frac{\partial^2 V_\theta}{\partial r \partial \theta} + \frac{1}{3} \frac{\partial^2 V_z}{\partial z \partial r} + \frac{1}{r^2} \frac{\partial^2 V_r}{\partial \theta^2} \right. \right. \\
&\quad \left. \left. - \frac{7}{3} \frac{1}{r^2} \frac{\partial V_\theta}{\partial \theta} + \frac{\partial^2 V_r}{\partial z^2} - \frac{4}{3} \frac{V_r}{r^2} \right) \right. \\
&\quad \left. + \frac{\partial \mu}{\partial r} \left(\frac{4}{3} \frac{\partial V_r}{\partial r} - \frac{2}{3} \frac{V_r}{r} - \frac{2}{3} \frac{1}{r} \frac{\partial V_\theta}{\partial \theta} - \frac{2}{3} \frac{\partial V_z}{\partial z} \right) \right. \\
&\quad \left. + \frac{\partial \mu}{\partial \theta} \left(\frac{1}{r} \frac{\partial V_\theta}{\partial r} + \frac{1}{r^2} \frac{\partial V_r}{\partial \theta} - \frac{V_\theta}{r^2} \right) + \frac{\partial \mu}{\partial z} \left(\frac{\partial V_r}{\partial z} + \frac{\partial V_z}{\partial r} \right) \right] \quad (1.9)
\end{aligned}$$

Polar Form of the θ - Momentum Equation

$$\begin{aligned}
& \rho \frac{\partial V_\theta}{\partial t} + \rho \left(V_r \frac{\partial V_\theta}{\partial r} + \frac{V_\theta}{r} \frac{\partial V_\theta}{\partial \theta} + \frac{V_r V_\theta}{r} + V_z \frac{\partial V_\theta}{\partial z} \right) + \frac{1}{\gamma M^2} \left(\frac{\rho}{r} \frac{\partial T}{\partial \theta} + \frac{T}{r} \frac{\partial \rho}{\partial \theta} \right) \\
&= \frac{1}{Re} \left[\mu \left(\frac{\partial^2 V_\theta}{\partial r^2} + \frac{1}{3} \frac{1}{r} \frac{\partial^2 V_r}{\partial \theta \partial r} + \frac{4}{3} \frac{1}{r^2} \frac{\partial^2 V_\theta}{\partial \theta^2} + \frac{7}{3} \frac{1}{r^2} \frac{\partial V_r}{\partial \theta} \right. \right. \\
&\quad \left. \left. + \frac{1}{3} \frac{1}{r} \frac{\partial^2 V_z}{\partial \theta \partial z} + \frac{\partial^2 V_\theta}{\partial z^2} + \frac{1}{r} \frac{\partial V_\theta}{\partial r} - \frac{V_\theta}{r^2} \right) \right. \\
&\quad \left. + \frac{\partial \mu}{\partial r} \left(\frac{\partial V_\theta}{\partial r} + \frac{1}{r} \frac{\partial V_r}{\partial \theta} - \frac{V_\theta}{r} \right) \right. \\
&\quad \left. + \frac{\partial \mu}{\partial \theta} \left(\frac{4}{3} \frac{1}{r^2} \frac{\partial V_\theta}{\partial \theta} + \frac{4}{3} \frac{V_r}{r^2} - \frac{2}{3} \frac{1}{r} \frac{\partial V_r}{\partial r} - \frac{2}{3} \frac{1}{r} \frac{\partial V_z}{\partial z} \right) \right. \\
&\quad \left. + \frac{\partial \mu}{\partial z} \left(\frac{\partial V_\theta}{\partial z} + \frac{1}{r} \frac{\partial V_z}{\partial \theta} \right) \right] \quad (1.10)
\end{aligned}$$

Polar Form of the z - Momentum Equation

$$\begin{aligned}
& \rho \frac{\partial V_z}{\partial t} + \rho \left(V_r \frac{\partial V_z}{\partial r} + \frac{V_\theta}{r} \frac{\partial V_z}{\partial \theta} + V_z \frac{\partial V_z}{\partial z} \right) + \frac{1}{\gamma M^2} \left(\rho \frac{\partial T}{\partial z} + T \frac{\partial \rho}{\partial z} \right) \\
&= \frac{1}{Re} \left[\mu \left(\frac{\partial^2 V_z}{\partial r^2} + \frac{1}{r^2} \frac{\partial^2 V_z}{\partial \theta^2} + \frac{4}{3} \frac{\partial^2 V_z}{\partial z^2} + \frac{1}{3} \frac{\partial^2 V_r}{\partial r \partial z} + \frac{1}{r} \frac{\partial V_z}{\partial r} \right. \right. \\
&\quad \left. \left. + \frac{1}{3} \frac{1}{r} \frac{\partial V_r}{\partial z} + \frac{1}{3} \frac{1}{r} \frac{\partial^2 V_\theta}{\partial \theta \partial z} \right) \right. \\
&\quad \left. + \frac{\partial \mu}{\partial r} \left(\frac{\partial V_z}{\partial r} + \frac{\partial V_r}{\partial z} \right) + \frac{\partial \mu}{\partial \theta} \left(\frac{1}{r^2} \frac{\partial V_z}{\partial \theta} + \frac{1}{r} \frac{\partial V_\theta}{\partial z} \right) \right. \\
&\quad \left. + \frac{\partial \mu}{\partial z} \left(\frac{4}{3} \frac{\partial V_z}{\partial z} - \frac{2}{3} \frac{\partial V_r}{\partial r} - \frac{2}{3} \frac{V_r}{r} - \frac{2}{3} \frac{1}{r} \frac{\partial V_\theta}{\partial \theta} \right) \right] \quad (1.11)
\end{aligned}$$

Polar Form of the Energy Equation

$$\begin{aligned}
& \rho \frac{\partial T}{\partial t} + \rho \left(V_r \frac{\partial T}{\partial r} + \frac{V_\theta}{r} \frac{\partial T}{\partial \theta} + V_z \frac{\partial T}{\partial z} \right) + (\gamma - 1) \rho T \left(\frac{\partial V_r}{\partial r} + \frac{V_r}{r} + \frac{1}{r} \frac{\partial V_\theta}{\partial \theta} + \frac{\partial V_z}{\partial z} \right) \\
&= \frac{\gamma}{Re Pr} \left[\kappa \left(\frac{\partial^2 T}{\partial r^2} + \frac{1}{r} \frac{\partial T}{\partial r} + \frac{1}{r^2} \frac{\partial^2 T}{\partial \theta^2} + \frac{\partial^2 T}{\partial z^2} \right) + \frac{\partial \kappa}{\partial r} \frac{\partial T}{\partial r} + \frac{1}{r^2} \frac{\partial \kappa}{\partial \theta} \frac{\partial T}{\partial \theta} + \frac{\partial \kappa}{\partial z} \frac{\partial T}{\partial z} \right] \\
&+ \frac{M^2 \gamma (\gamma - 1)}{Re} \mu \left[\frac{\partial V_r}{\partial r} \left(\frac{4}{3} \frac{\partial V_r}{\partial r} - \frac{2}{3} \frac{V_r}{r} - \frac{2}{3} \frac{1}{r} \frac{\partial V_\theta}{\partial \theta} - \frac{2}{3} \frac{\partial V_z}{\partial z} \right) \right. \\
&\quad \left. + \left(\frac{\partial V_r}{\partial \theta} + \frac{\partial V_\theta}{\partial r} - \frac{V_\theta}{r} \right) \left(\frac{\partial V_\theta}{\partial r} + \frac{1}{r} \frac{\partial V_r}{\partial \theta} - \frac{V_r}{r} \right) \right. \\
&\quad \left. + \left(\frac{1}{r} \frac{\partial V_\theta}{\partial \theta} + \frac{V_r}{r} \right) \left(\frac{4}{3} \frac{1}{r} \frac{\partial V_\theta}{\partial \theta} + \frac{4}{3} \frac{V_r}{r} - \frac{2}{3} \frac{\partial V_r}{\partial r} - \frac{2}{3} \frac{\partial V_z}{\partial z} \right) \right. \\
&\quad \left. + \left(\frac{\partial V_\theta}{\partial z} + \frac{1}{r} \frac{\partial V_z}{\partial \theta} \right) \left(\frac{\partial V_\theta}{\partial z} + \frac{1}{r} \frac{\partial V_z}{\partial \theta} \right) \right. \\
&\quad \left. + \frac{\partial V_z}{\partial z} \left(\frac{4}{3} \frac{\partial V_z}{\partial z} - \frac{2}{3} \frac{\partial V_r}{\partial r} - \frac{2}{3} \frac{V_r}{r} - \frac{2}{3} \frac{1}{r} \frac{\partial V_\theta}{\partial \theta} \right) + \left(\frac{\partial V_r}{\partial z} + \frac{\partial V_z}{\partial r} \right) \left(\frac{\partial V_z}{\partial r} + \frac{\partial V_r}{\partial z} \right) \right] \quad (1.12)
\end{aligned}$$

1.5 Linearized Navier-Stokes

The polar form of each equation starting from equation (1.7) is obtained by replacing the terms with the relations in Appendix A. Once the equations are in polar form, the first assumptions that we make in order to linearize the equations are that: 1) products of fluctuating quantities are negligible; 2) all variables have the form: $\phi = \bar{\phi} + \phi'$; 3) $\bar{\rho}$, \bar{T} and \bar{V}_z are all potentially non-zero and functions only of r ; and 4) $\bar{V}_r = \bar{V}_\theta = 0$. Having all these terms allows for a parallel representation of flow in a jet, however we will also include terms obtained from allowing $\bar{\rho}$, \bar{T} , \bar{V}_z and \bar{V}_r in the inviscid or left hand side to be functions of z as well and $\bar{V}_r \neq 0$. These new terms provide the non-parallel form of the equations and can be used in a separate code based on the Parabolized Stability equations (PSE). Each of the equations is simplified by introducing these assumptions, canceling out terms that become negligible or equal to zero and subtracting the mean form of the equations. In the next sections we will see the linearized form obtained for each component of the Navier-Stokes equations.

1.5.1 Continuity Equation

$$\begin{aligned} \frac{\partial \rho'}{\partial t} + \bar{V}_r \frac{\partial \rho'}{\partial r} + V_r' \frac{\partial \bar{\rho}}{\partial r} + \bar{V}_z \frac{\partial \rho'}{\partial z} + V_z' \frac{\partial \bar{\rho}}{\partial z} + \bar{\rho} \frac{\partial V_r'}{\partial r} + \rho' \frac{\partial \bar{V}_r}{\partial r} \\ + \bar{\rho} \frac{V_r'}{r} + \rho' \frac{\bar{V}_r}{r} + \frac{\bar{\rho}}{r} \frac{\partial V_\theta'}{\partial r} + \bar{\rho} \frac{\partial V_z'}{\partial z} + \rho' \frac{\partial \bar{V}_z}{\partial z} = 0 \end{aligned} \quad (1.13)$$

1.5.2 r - Momentum Equation

The inviscid terms (or left hand side, LHS_r) of the r -Momentum Equation reduce to:

$$\begin{aligned} \bar{\rho} \frac{\partial V_r'}{\partial t} + \bar{\rho} \bar{V}_r \frac{\partial V_r'}{\partial r} + \bar{\rho} V_r' \frac{\partial \bar{V}_r}{\partial r} + \rho' \bar{V}_r \frac{\partial \bar{V}_r}{\partial r} + \bar{\rho} \bar{V}_z \frac{\partial V_r'}{\partial z} + \bar{\rho} V_z' \frac{\partial \bar{V}_r}{\partial z} \\ + \rho' \bar{V}_z \frac{\partial \bar{V}_r}{\partial z} + \frac{1}{\gamma M^2} \left(\bar{\rho} \frac{\partial T'}{\partial r} + \rho' \frac{\partial \bar{T}}{\partial r} + \bar{T} \frac{\partial \rho'}{\partial r} + T' \frac{\partial \bar{\rho}}{\partial r} \right) \\ = \frac{1}{Re} RHS_r \end{aligned} \quad (1.14)$$

Here RHS_r (right hand side) contains the viscous terms which are obtained by neglecting nonparallel terms:

$$\begin{aligned}
RHS_r &= \frac{4}{3}\bar{\mu}\frac{\partial^2 V_r'}{\partial r^2} + \frac{4}{3}\frac{\bar{\mu}}{r}\frac{\partial V_r'}{\partial r} + \frac{1}{3}\frac{\bar{\mu}}{r}\frac{\partial^2 V_\theta'}{\partial r\partial\theta} + \frac{1}{3}\bar{\mu}\frac{\partial^2 V_z'}{\partial z\partial r} + \frac{\bar{\mu}}{r^2}\frac{\partial^2 V_r'}{\partial\theta^2} \\
&- \frac{7}{3}\frac{\bar{\mu}}{r^2}\frac{\partial V_\theta'}{\partial\theta} + \bar{\mu}\frac{\partial^2 V_r'}{\partial z^2} - \frac{4}{3}\bar{\mu}\frac{V_r'}{r^2} + \frac{4}{3}\frac{\partial\bar{\mu}}{\partial r}\frac{\partial V_r'}{\partial r} - \frac{2}{3}\frac{\partial\bar{\mu}}{\partial r}\frac{V_r'}{r} \\
&- \frac{2}{3}\frac{1}{r}\frac{\partial\bar{\mu}}{\partial r}\frac{\partial V_\theta'}{\partial\theta} - \frac{2}{3}\frac{\partial\bar{\mu}}{\partial r}\frac{\partial V_z'}{\partial z} + \frac{\partial\mu'}{\partial z}\frac{\partial\bar{V}_z}{\partial r}
\end{aligned} \tag{1.15}$$

1.5.3 θ - Momentum Equation

The non-viscous terms (or left hand side, LHS_θ) of the θ -Momentum Equation reduce to:

$$\begin{aligned}
\bar{\rho}\frac{\partial V_\theta'}{\partial t} &+ \bar{\rho}\bar{V}_r\frac{\partial V_\theta'}{\partial r} + \bar{\rho}V_\theta'\frac{\bar{V}_r}{r} + \bar{\rho}\bar{V}_z\frac{\partial V_\theta'}{\partial z} + \frac{1}{\gamma M^2}\left(\frac{\bar{\rho}}{r}\frac{\partial T'}{\partial\theta} + \frac{\bar{T}}{r}\frac{\partial\rho'}{\partial\theta}\right) \\
&= \frac{1}{Re}RHS_\theta
\end{aligned} \tag{1.16}$$

RHS_θ , contains the viscous terms:

$$\begin{aligned}
RHS_\theta &= \bar{\mu}\frac{\partial^2 V_\theta'}{\partial r^2} + \frac{1}{3}\frac{\bar{\mu}}{r}\frac{\partial^2 V_r'}{\partial\theta\partial r} + \frac{4}{3}\frac{\bar{\mu}}{r^2}\frac{\partial^2 V_\theta'}{\partial\theta^2} + \frac{7}{3}\frac{\bar{\mu}}{r^2}\frac{\partial V_r'}{\partial\theta} \\
&+ \frac{1}{3}\frac{\bar{\mu}}{r}\frac{\partial^2 V_z'}{\partial\theta\partial z} + \bar{\mu}\frac{\partial^2 V_\theta'}{\partial z^2} + \frac{\bar{\mu}}{r}\frac{\partial V_\theta'}{\partial r} - \frac{\bar{\mu}}{r^2}V_\theta' \\
&+ \frac{\partial\bar{\mu}}{\partial r}\frac{\partial V_\theta'}{\partial r} + \frac{1}{r}\frac{\partial\bar{\mu}}{\partial r}\frac{\partial V_r'}{\partial\theta} - \frac{\partial\bar{\mu}}{\partial r}\frac{V_\theta'}{r}
\end{aligned} \tag{1.17}$$

1.5.4 z - Momentum Equation

The non-viscous terms (or left hand side, LHS_z) of the z -Momentum Equation reduce to:

$$\begin{aligned}
& \bar{\rho} \frac{\partial V'_z}{\partial t} + \bar{\rho} \bar{V}_r \frac{\partial V'_z}{\partial r} + \bar{\rho} V'_r \frac{\partial \bar{V}_z}{\partial r} + \rho' \bar{V}_r \frac{\partial \bar{V}_z}{\partial r} + \bar{\rho} \bar{V}_z \frac{\partial V'_z}{\partial z} + \bar{\rho} V'_z \frac{\partial \bar{V}_z}{\partial z} \\
& + \rho' \bar{V}_z \frac{\partial \bar{V}_z}{\partial z} + \frac{1}{\gamma M^2} \left(\bar{\rho} \frac{\partial T'}{\partial z} + \rho' \frac{\partial \bar{T}}{\partial z} + \bar{T} \frac{\partial \rho'}{\partial z} + T' \frac{\partial \bar{\rho}}{\partial z} \right) \\
& = \frac{1}{Re} RHS_z
\end{aligned} \tag{1.18}$$

RHS_z , contains viscous terms:

$$\begin{aligned}
RHS_z &= \bar{\mu} \frac{\partial^2 V'_z}{\partial r^2} + \mu' \frac{\partial^2 \bar{V}_z}{\partial r^2} + \frac{\bar{\mu}}{r^2} \frac{\partial^2 V'_z}{\partial \theta^2} + \frac{4}{3} \bar{\mu} \frac{\partial^2 V'_z}{\partial z^2} + \frac{1}{3} \bar{\mu} \frac{\partial^2 V'_r}{\partial r \partial z} + \frac{\bar{\mu}}{r} \frac{\partial V'_z}{\partial r} \\
&+ \frac{\mu'}{r} \frac{\partial \bar{V}_z}{\partial r} + \frac{1}{3} \frac{\bar{\mu}}{r} \frac{\partial V'_r}{\partial z} + \frac{1}{3} \frac{\bar{\mu}}{r} \frac{\partial^2 V'_\theta}{\partial \theta \partial z} + \frac{\partial \bar{\mu}}{\partial r} \frac{\partial V'_z}{\partial r} + \frac{\partial \mu'}{\partial r} \frac{\partial \bar{V}_z}{\partial r} \\
&+ \frac{\partial \bar{\mu}}{\partial r} \frac{\partial V'_r}{\partial z}
\end{aligned} \tag{1.19}$$

1.5.5 Energy Equation

The non-viscous terms (or left hand side) of the Energy Equation reduce to:

$$\begin{aligned}
& \bar{\rho} \frac{\partial T'}{\partial t} + \bar{\rho} \bar{V}_r \frac{\partial T'}{\partial r} + \bar{\rho} V'_r \frac{\partial \bar{T}}{\partial r} + \rho' \bar{V}_r \frac{\partial \bar{T}}{\partial r} + \bar{\rho} \bar{V}_z \frac{\partial T'}{\partial z} + \bar{\rho} V'_z \frac{\partial \bar{T}}{\partial z} + \rho' \bar{V}_z \frac{\partial \bar{T}}{\partial z} \\
& + (\gamma - 1) \left(\bar{\rho} \bar{T} \frac{\partial V'_r}{\partial r} + \bar{\rho} T' \frac{\partial \bar{V}_r}{\partial r} + \rho' \bar{T} \frac{\partial \bar{V}_r}{\partial r} + \bar{\rho} \bar{T} \frac{V'_r}{r} + \bar{\rho} T' \frac{\bar{V}_r}{r} \right) \\
& + (\gamma - 1) \left(\rho' \bar{T} \frac{\bar{V}_r}{r} + \frac{\bar{\rho} \bar{T}}{r} \frac{\partial V'_\theta}{\partial \theta} + \bar{\rho} \bar{T} \frac{\partial V'_z}{\partial z} + \bar{\rho} T' \frac{\partial \bar{V}_z}{\partial z} + \rho' \bar{T} \frac{\partial \bar{V}_z}{\partial z} \right) \\
& = \frac{\gamma}{Re Pr} \nabla \cdot (\kappa (\nabla T)) + \frac{M^2 \gamma (\gamma - 1)}{Re} \underline{\underline{T}} \cdot (\nabla \underline{u})
\end{aligned} \tag{1.20}$$

The main terms on the RHS , reduce to:

$$\begin{aligned}
\nabla \cdot (\kappa (\nabla T)) &= \frac{\partial \bar{\kappa}}{\partial r} \frac{\partial T'}{\partial r} + \frac{\partial \kappa'}{\partial r} \frac{\partial \bar{T}}{\partial r} + \bar{\kappa} \frac{\partial^2 T'}{\partial r^2} + \kappa' \frac{\partial^2 \bar{T}}{\partial r^2} \\
&+ \frac{\bar{\kappa}}{r} \frac{\partial T'}{\partial r} + \frac{\kappa'}{r} \frac{\partial \bar{T}}{\partial r} + \frac{\bar{\kappa}}{r^2} \frac{\partial^2 T'}{\partial \theta^2} + \bar{\kappa} \frac{\partial^2 T'}{\partial z^2}
\end{aligned} \tag{1.21}$$

$$\underline{\tau} \cdot (\nabla \underline{u}) = \mu' \left(\frac{\partial \bar{V}_z}{\partial r} \right)^2 + 2\bar{\mu} \frac{\partial \bar{V}_z}{\partial r} \frac{\partial V'_z}{\partial r} + 2\bar{\mu} \frac{\partial \bar{V}_z}{\partial r} \frac{\partial V'_r}{\partial z} \quad (1.22)$$

1.6 Final Form of Equations used in program

We replace all the fluctuations of the variables, density (ρ'), radial velocity (V'_r), angular velocity (V'_θ), streamwise velocity (V'_z) and temperature (T), with the following normal mode form:

$$\phi' = \hat{\phi} e^{i(\alpha z + m\theta - \omega t)} \quad (1.23)$$

This leads to a linear system of the form:

$$(L_i + L_{iD} - L_V - L_{VD})\hat{\phi} = \omega K \hat{\phi} \quad (1.24)$$

Where L_i contains the inviscid terms without derivatives of $\hat{\phi}$ with respect to r , L_{iD} contains all the inviscid terms with derivatives of $\hat{\phi}$ with respect to r , L_V contains all the viscous terms without derivatives of $\hat{\phi}$ with respect to r , L_{VD} contains all the viscous terms with derivatives of $\hat{\phi}$ with respect to r , and K contains all the terms that are multiplied by the frequency ω . Here ϕ represents the array containing each of the five variables of our NSEs at each n -location along the r -axis. Also we can define the parabolized stability equations (PSE) by:

$$M \frac{d\hat{\phi}}{dz} = (\omega K - L - L')\hat{\phi} \quad (1.25)$$

Where $L = L_i + L_{iD} - L_V - L_{VD}$, and L' and M contain the non-parallel and additional PSE terms that arise from including $\bar{V}_r \neq 0$ and derivatives with respect to z . This second linear system can be solved by iteration to determine the flow at different z -locations.

1.6.1 Continuity Equation

Non-Viscous Terms

$$\begin{aligned}
L_i \hat{\phi} &= [i\alpha \bar{V}_z] \hat{\rho} + \left[\frac{\partial \bar{\rho}}{\partial r} + \frac{\bar{\rho}}{r} \right] \hat{V}_r + \left[\frac{im\bar{\rho}}{r} \right] \hat{V}_\theta + [i\alpha \bar{\rho}] \hat{V}_z \\
L_{iD} \hat{\phi} &= [\bar{\rho} D] \hat{V}_r \\
K \hat{\phi} &= [i] \hat{\rho}
\end{aligned} \tag{1.26}$$

PSE Terms

$$\begin{aligned}
L' \hat{\phi} &= \left[\bar{V}_r D + \frac{\partial \bar{V}_r}{\partial r} + \frac{\bar{V}_r}{r} + \frac{\partial \bar{V}_z}{\partial z} \right] \hat{\rho} + \left[\frac{\partial \bar{\rho}}{\partial z} \right] \hat{V}_z \\
M \frac{\partial \hat{\phi}}{\partial z} &= [\bar{V}_z] \frac{\partial \hat{\rho}}{\partial z} + [\bar{\rho}] \frac{\partial \hat{V}_z}{\partial z}
\end{aligned} \tag{1.27}$$

1.6.2 r - Momentum Equation

Non-Viscous Terms

$$\begin{aligned}
L_i \hat{\phi} &= \left[\frac{1}{\gamma M^2} \frac{\partial \bar{T}}{\partial r} \right] \hat{\rho} + [i\alpha \bar{\rho} \bar{V}_z] \hat{V}_r + \left[\frac{1}{\gamma M^2} \frac{\partial \bar{\rho}}{\partial r} \right] \hat{T} \\
L_{iD} \hat{\phi} &= \left[\frac{\bar{T} D}{\gamma M^2} \right] \hat{\rho} + \left[\frac{\bar{\rho} D}{\gamma M^2} \right] \hat{T} \\
K \hat{\phi} &= [i\bar{\rho}] \hat{V}_r
\end{aligned} \tag{1.28}$$

PSE Terms

$$\begin{aligned}
L' \hat{\phi} &= \left[\bar{V}_r \frac{\partial \bar{V}_r}{\partial r} + \bar{V}_z \frac{\partial \bar{V}_r}{\partial z} \right] \hat{\rho} + \left[\bar{\rho} \bar{V}_r D + \bar{\rho} \frac{\partial \bar{V}_r}{\partial r} \right] \hat{V}_r + \left[\bar{\rho} \frac{\partial \bar{V}_r}{\partial z} \right] \hat{V}_z \\
M \frac{\partial \hat{\phi}}{\partial z} &= [\bar{\rho} \bar{V}_z] \frac{\partial \hat{V}_r}{\partial z}
\end{aligned} \tag{1.29}$$

Viscous Terms

$$\begin{aligned}
L_V \hat{\phi} &= \frac{1}{Re} \left[-\frac{m^2}{r^2} \bar{\mu} - \alpha^2 \bar{\mu} - \frac{4}{3} \frac{\bar{\mu}}{r^2} - \frac{2}{3} \frac{1}{r} \frac{\partial \bar{\mu}}{\partial r} \right] \hat{V}_r + \frac{1}{Re} \left[-\frac{7}{3} \frac{im}{r^2} \bar{\mu} - \frac{2}{3} \frac{im}{r} \frac{\partial \bar{\mu}}{\partial r} \right] \hat{V}_\theta \\
&\quad - \frac{1}{Re} \left[\frac{2}{3} i\alpha \frac{\partial \bar{\mu}}{\partial r} \right] \hat{V}_z + \frac{1}{Re} \left[i\alpha \frac{\partial \bar{V}_z}{\partial r} \frac{\partial \mu}{\partial T} \right] \hat{T} \\
L_{VD} \hat{\phi} &= \frac{1}{Re} \left[\frac{4}{3} \bar{\mu} D^2 + \frac{4}{3} \frac{\bar{\mu}}{r} D + \frac{4}{3} \frac{\partial \bar{\mu}}{\partial r} D \right] \hat{V}_r + \frac{1}{Re} \left[\frac{1}{3} \frac{im}{r} \bar{\mu} D \right] \hat{V}_\theta \\
&\quad + \frac{1}{Re} \left[\frac{i\alpha}{3} \bar{\mu} D \right] \hat{V}_z
\end{aligned} \tag{1.30}$$

1.6.3 θ -Momentum Equation

Non-Viscous Terms

$$\begin{aligned}
L_i \hat{\phi} &= \left[\frac{im}{\gamma M^2} \frac{\bar{T}}{r} \right] \hat{\rho} + [i\alpha \bar{\rho} \bar{V}_z] \hat{V}_\theta + \left[\frac{im}{\gamma M^2} \frac{\bar{\rho}}{r} \right] \hat{T} \\
K \hat{\phi} &= [i\bar{\rho}] \hat{V}_\theta
\end{aligned} \tag{1.31}$$

PSE Terms

$$\begin{aligned}
L' \hat{\phi} &= \left[\bar{\rho} \bar{V}_r D + \bar{\rho} \frac{\bar{V}_r}{r} \right] \hat{V}_\theta \\
M \frac{\partial \hat{\phi}}{\partial z} &= [\bar{\rho} \bar{V}_z] \frac{\partial \hat{V}_\theta}{\partial z}
\end{aligned} \tag{1.32}$$

Viscous Terms

$$\begin{aligned}
L_V \hat{\phi} &= \frac{1}{Re} \left[\frac{7im}{3r^2} \bar{\mu} + \frac{im}{r} \frac{\partial \bar{\mu}}{\partial r} \right] \hat{V}_r + \frac{1}{Re} \left[-\frac{4m^2}{3r^2} \bar{\mu} - \alpha^2 \bar{\mu} - \frac{\bar{\mu}}{r^2} - \frac{1}{r} \frac{\partial \bar{\mu}}{\partial r} \right] \hat{V}_\theta \\
&\quad - \frac{1}{Re} \left[\frac{1}{3} m \alpha \frac{\partial \bar{\mu}}{\partial r} \right] \hat{V}_z \\
L_{VD} \hat{\phi} &= \frac{1}{Re} \left[\frac{1}{3} \frac{im}{r} \bar{\mu} D \right] \hat{V}_r + \frac{1}{Re} \left[\bar{\mu} D^2 + \frac{\bar{\mu}}{r} D + \frac{\partial \bar{\mu}}{\partial r} D \right] \hat{V}_\theta
\end{aligned} \tag{1.33}$$

1.6.4 z - Momentum Equation

Non-viscous Terms

$$\begin{aligned}
L \hat{\phi} &= \left[\frac{i\alpha \bar{T}}{\gamma M^2} \right] \hat{\rho} + \left[\bar{\rho} \frac{\partial \bar{V}_z}{\partial r} \right] \hat{V}_r + [i\alpha \bar{\rho} \bar{V}_z] \hat{V}_z + \left[\frac{i\alpha \bar{\rho}}{\gamma M^2} \right] \hat{T} \\
K \hat{\phi} &= [i\bar{\rho}] \hat{V}_z
\end{aligned} \tag{1.34}$$

PSE Terms

$$\begin{aligned}
L' \hat{\phi} &= \left[\bar{V}_r \frac{\partial \bar{V}_z}{\partial r} + \bar{V}_z \frac{\partial \bar{V}_z}{\partial z} + \frac{1}{\gamma M^2} \left(\frac{\partial \bar{T}}{\partial z} \right) \right] \hat{\rho} + \left[\bar{\rho} \bar{V}_r D + \bar{\rho} \frac{\partial \bar{V}_z}{\partial z} \right] \hat{V}_z + \frac{1}{\gamma M^2} \left[\frac{\partial \bar{\rho}}{\partial z} \right] \hat{T} \\
M \frac{\partial \hat{\phi}}{\partial z} &= \left[\frac{\bar{T}}{\gamma M^2} \right] \frac{\partial \hat{\rho}}{\partial z} + [\bar{\rho} \bar{V}_z] \frac{\partial \hat{V}_z}{\partial z} + \left[\frac{\bar{\rho}}{\gamma M^2} \right] \frac{\partial \hat{T}}{\partial z}
\end{aligned} \tag{1.35}$$

Viscous Terms

$$\begin{aligned}
L_V \hat{\phi} &= \frac{1}{Re} \left[\frac{1}{3} \frac{i\alpha}{r} \bar{\mu} + i\alpha \frac{\partial \bar{\mu}}{\partial r} \right] \hat{V}_r + \frac{1}{Re} \left[-\frac{1}{3} \frac{m\alpha}{r} \bar{\mu} \right] \hat{V}_\theta + \frac{1}{Re} \left[-\frac{m^2}{r^2} \bar{\mu} - \frac{4}{3} \alpha^2 \bar{\mu} \right] \hat{V}_z \\
&+ \frac{1}{Re} \left[\frac{\partial^2 \bar{V}_z}{\partial r^2} \frac{\partial \mu}{\partial T} + \frac{1}{r} \frac{\partial \mu}{\partial T} \frac{\partial \bar{V}_z}{\partial r} \right] \hat{T} \\
L_{VD} \hat{\phi} &= \frac{1}{Re} \left[\frac{i\alpha}{3} \bar{\mu} D \right] \hat{V}_r + \frac{1}{Re} \left[\bar{\mu} D^2 + \frac{\bar{\mu}}{r} D + \frac{\partial \bar{\mu}}{\partial r} D \right] \hat{V}_z \\
&+ \frac{1}{Re} \left[\frac{\partial \mu}{\partial T} \frac{\partial \bar{V}_z}{\partial r} D \right] \hat{T}
\end{aligned} \tag{1.36}$$

1.6.5 Energy Equation

Non-Viscous Terms

$$\begin{aligned}
L \hat{\phi} &= \left[\bar{\rho} \frac{\partial \bar{T}}{\partial r} + \frac{(\gamma-1)}{r} \bar{\rho} \bar{T} \right] \hat{V}_r + \left[(\gamma-1) \frac{in}{r} \bar{\rho} \bar{T} \right] \hat{V}_\theta \\
&+ [(\gamma-1) i\alpha \bar{\rho} \bar{T}] \hat{V}_z + [i\alpha \bar{\rho} \bar{V}_z] \hat{T} \\
L_D \hat{\phi} &= [(\gamma-1) \bar{\rho} \bar{T} D] \hat{V}_r \\
K \hat{\phi} &= [i\bar{\rho}] \hat{T}
\end{aligned} \tag{1.37}$$

PSE Terms

$$\begin{aligned}
L' \hat{\phi} &= \left[\bar{V}_r \frac{\partial \bar{T}}{\partial r} + \bar{V}_z \frac{\partial \bar{T}}{\partial z} + (\gamma-1) \bar{T} \left(\frac{\partial \bar{V}_r}{\partial r} + \frac{\bar{V}_r}{r} + \frac{\partial \bar{V}_z}{\partial z} \right) \right] \hat{\rho} \\
&+ \left[\bar{\rho} \frac{\partial \bar{T}}{\partial z} \right] \hat{V}_z + \left[\bar{\rho} \bar{V}_r D + (\gamma-1) \bar{\rho} \left(\frac{\partial \bar{V}_r}{\partial r} + \frac{\bar{V}_r}{r} + \frac{\partial \bar{V}_z}{\partial z} \right) \right] \hat{T} \\
M \frac{\partial \hat{\phi}}{\partial z} &= [(\gamma-1) \bar{\rho} \bar{T}] \frac{\partial \hat{V}_z}{\partial z} + [\bar{\rho} \bar{V}_z] \frac{\partial \hat{T}}{\partial z}
\end{aligned} \tag{1.38}$$

Viscous Terms

$$\begin{aligned}
L_V \hat{\phi} &= \frac{M^2 \gamma (\gamma - 1)}{Re} \left[2i\alpha \bar{\mu} \frac{\partial \bar{V}_z}{\partial r} \right] \hat{V}_r + \frac{M^2 \gamma (\gamma - 1)}{Re} \left[\left(\frac{\partial \bar{V}_z}{\partial r} \right)^2 \frac{\partial \mu}{\partial T} \right] \hat{T} \\
&+ \frac{\gamma}{Pr Re} \left[\frac{\partial^2 \bar{T}}{\partial r^2} \frac{\partial \kappa}{\partial T} + \frac{1}{r} \frac{\partial \kappa}{\partial T} \frac{\partial \bar{T}}{\partial r} - \frac{m^2}{r} \bar{\kappa} - \alpha^2 \bar{\kappa} \right] \hat{T} \quad (1.39) \\
L_{VD} \hat{\phi} &= \frac{M^2 \gamma (\gamma - 1)}{Re} \left[2\bar{\mu} \frac{\partial \bar{V}_z}{\partial r} D \right] \hat{V}_z \\
&+ \frac{\gamma}{Pr Re} \left[\frac{\partial \bar{\kappa}}{\partial r} D + \frac{\partial \kappa}{\partial T} \frac{\partial \bar{T}}{\partial r} D + \bar{\kappa} D^2 + \frac{\bar{\kappa}}{r} D \right] \hat{T}
\end{aligned}$$

Now we can solve equation 1.24 for a particular value of the wavenumber α at a particular z -location, and thus find the most temporally unstable disturbance.

2 Numerical Method and Differentiation Schemes

2.1 Grid

In order to have a grid that is heavily concentrated near the jet shear layer ($r = r_j$), but less so at the far field ($r \rightarrow \infty$), we use a stretched grid obtained from applying the following relation to an equally distributed independent variable, η :

$$r = r_J + L \frac{\sinh c\eta}{\sinh c} \quad (2.1)$$

where: $r_J = 0.5$, $-\eta_0 < \eta < 1$ and $\eta = \eta_0$ is where $r = 0$. The parameters L and c define how much the grid is stretched and where it will be most densely packed. They will have to be varied in order to find the combination that provides the best grid for particular cases. Unless otherwise stated we take $c = 5.0$ because it effectively concentrates grid points near r_J where we generally need the most resolution.

2.2 Differentiation Schemes

The differentiation scheme used to find the derivatives of the main flow quantities with respect to r is a very important part of the code. We compare a sixth order finite difference scheme from Lele [2] with Canuto's et al ([1, page 69]) Chebyshev scheme. This scheme uses a different algebraic grid mapping that depends only on one parameter, L . The sixth order scheme is detailed in the following section.

2.2.1 6th Order Modified Padé

A series of higher order modified Padé schemes were derived by Lele using a uniformly distributed independent variable, η , and obtaining from the following matrix systems for the first and second derivatives.

$$\begin{aligned}
\phi'_{j+1} + a_1\phi'_j + \phi'_{j-1} &= b_1 \frac{\phi_{j+1} - \phi_{j-1}}{2\Delta\eta} + c_1 \frac{\phi_{j+2} - \phi_{j-2}}{4\Delta\eta} \\
\phi''_{j+1} + a_2\phi''_j + \phi''_{j-1} &= b_2 \frac{\phi_{j+1} - 2\phi_j + \phi_{j-1}}{\Delta\eta^2} + c_2 \frac{\phi_{j+2} - 2\phi_j + \phi_{j-2}}{4\Delta\eta^2}
\end{aligned} \tag{2.2}$$

where:

$$\begin{aligned}
\phi' &= \frac{\partial\phi}{\partial\eta} & \phi'' &= \frac{\partial^2\phi}{\partial\eta^2} \\
b_1 &= \frac{2 + 4a_1}{3} & c_1 &= \frac{4 - a_1}{3} \\
b_2 &= \frac{4a_2 - 4}{3} & c_2 &= \frac{10 - a_2}{3}
\end{aligned}$$

If we take $a_1 = 3$ and $a_2 = 4$ we obtain a 6th-order finite difference scheme that can be solved implicitly to find ϕ'_{j+1} and ϕ''_{j+1} . We also know that since r is not evenly distributed and is a function of η , then:

$$\frac{\partial\phi}{\partial r} = \frac{1}{h'} \frac{\partial\phi}{\partial\eta} \quad \text{and} \quad \frac{\partial^2\phi}{\partial r^2} = \frac{1}{h'^2} \frac{\partial^2\phi}{\partial\eta^2} + \frac{h''}{h'^3} \frac{\partial\phi}{\partial\eta} \tag{2.3}$$

where: $h' = \frac{\partial r}{\partial\eta}$ and $h'' = \frac{\partial^2 r}{\partial\eta^2}$.

For the grid discussed in the previous section, we have that:

$$h' = LC \frac{\cosh C\eta}{\sinh C} \quad \text{and} \quad h'' = LC^2 \frac{\sinh C\eta}{\sinh C} \tag{2.4}$$

We must also take into account that the derivatives at the end points ($r = 0$ and $r \rightarrow \infty$) are reduced to a third order asymmetric representation.

2.3 Boundary Conditions

In order to solve the linear system we must define values of the perturbations, $\hat{\phi}$, at the boundaries. According to Lewis and Bellan's study [4] regarding the behaviour of Fourier coefficients in cylindrical coordinates, these boundary conditions at the centreline of the jet ($r = 0$) depend on the mode m . Also, in the far field the boundary conditions are that $\hat{\phi} \rightarrow 0$ when $r \rightarrow \infty$. In particular for each mode we must implement the following boundary conditions once our system has been defined and before the eigenvalue problem is solved.

For $|m| = 0$ and $r \rightarrow 0$:

$$\begin{aligned} D\hat{\rho} &\rightarrow 0 & D\hat{T} &\rightarrow 0 \\ \hat{V}_r &\rightarrow 0 & \hat{V}_\theta &\rightarrow 0 & D\hat{V}_z &\rightarrow 0 \end{aligned} \quad (2.5)$$

For $|m| = 1$ and $r \rightarrow 0$:

$$\begin{aligned} \hat{\rho} &\rightarrow 0 & \hat{T} &\rightarrow 0 \\ D\hat{V}_r &\rightarrow 0 & D\hat{V}_\theta &\rightarrow 0 & \hat{V}_z &\rightarrow 0 \end{aligned} \quad (2.6)$$

For $|m| > 1$ and $r \rightarrow 0$:

$$\begin{aligned} \hat{\rho} &\rightarrow 0 & \hat{T} &\rightarrow 0 \\ \hat{V}_r &\rightarrow 0 & \hat{V}_\theta &\rightarrow 0 & \hat{V}_z &\rightarrow 0 \end{aligned} \quad (2.7)$$

Now we can solve the temporal eigenvalue problem for a particular value of α_r , by inputting only the Reynolds Number, Mach Number, mode number and α_r , as well as the numerical parameters N (the number of grid points), L and C (for the sixth order differentiation scheme).

2.4 Secant Method

It is of great interest to obtain not only the temporal behaviour of disturbances but the spatial as well. This is why we develop a second code that iterates on α using a secant method until we find the prescribed value of ω_r

with $\omega_i = 0$ and hence the spatial behavior of the disturbances. This is done by using the following algorithm:

$$\alpha_{n+1} = \alpha_n - \frac{(\alpha_n - \alpha_{n-1})\epsilon_n}{\epsilon_n - \epsilon_{n-1}} \quad ; \quad \epsilon_n = \omega_n - \omega_{target} \quad (2.8)$$

The tolerance used for convergence was 10^{-8} for the error in ω_i which should be equal to zero. Usually the method will not require more than five iterations to reach this tolerance.

3 Validation Cases

Apart from checking the convergence of the differentiation schemes, we must also validate the final results obtained by the code. We do both by comparing with the results obtained from an inviscid code developed by Sandham and Luo [5], and the results found by Lessen and Singh [3] and Morris [6] for viscous incompressible flow. This way we check both the viscous and inviscid terms, however each of the previous codes work with different velocity profiles which are detailed in the following section.

3.1 Streamwise Velocity and Temperature Profiles.

The streamwise velocity profile of the fully developed jet used in references [3] and [6] is given by the following analytical equation:

Profile I

$$V_z = \frac{1}{(1+r)^2} \quad (3.1)$$

To compare with the results obtained from the inviscid code, we must use a jet profile defined at each z -position by:

Profile II

$$\begin{aligned} a &= 0.59 + 0.09 \tanh \sqrt{z} - 2.9 \\ \delta &= \frac{39 + 24z + 0.11z^4}{1000 + z^3} \\ V_z &= 0.5 \left[\tanh \left(\frac{r+a}{\delta} \right) - \tanh \left(\frac{r-a}{\delta} \right) \right] \end{aligned} \quad (3.2)$$

Here V_z and r are dimensionless. This profile was constructed to follow the spatial development of the experiment by Stromberg et al [7].

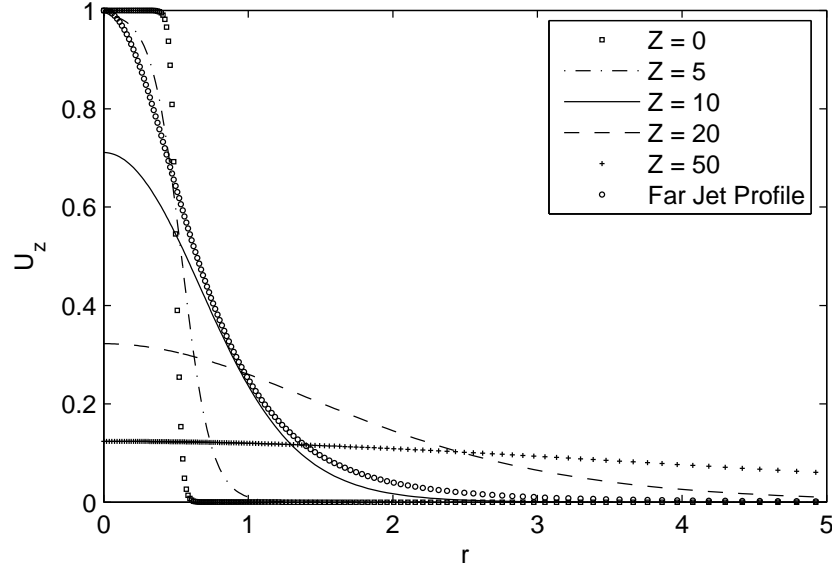


Figure 3.1: Streamwise Velocity Profiles developed.

Figure 3.1, shows how these profiles vary in the radial direction. The program is solved individually for each z -position therefore all though V_z is dependant on both z and r , it can be taken as a function only of r .

Temperature Profile

The mean temperature profile used throughout this investigation is given by:

$$\bar{T} = 1.0 + \left(\frac{(\gamma - 1)M^2}{2} \right) V_z(1 - V_z) \quad (3.3)$$

The mean density is defined as $\rho = 1/\bar{T}$.

3.2 Comparison with Incompressible Results

The first validation case, is the far jet profile (Profile I) used by Morris [6] and by Lessen and Singh [3]. We use it to validate the viscous terms of the equations since the compressible terms become negligible. At a $Re = 80$, with $m = 0$ and $\alpha = 0.2322 + i0.0666$ Morris found that $\omega_r = 0.2$ and $\omega_i = 0$.

We use our code with these input parameters and compare the values of ω obtained with each differentiation scheme and the convergence of each of these for different values of the parameter L . To avoid singularities the Mach number used throughout this report to compare with incompressible results is $M = 0.1$.

Tables 1 and 2, show the results obtained for ω_r and ω_i respectively, using the sixth order finite difference scheme, denoted FDS. For values of: $20 \leq L \leq 40$ and $N \geq 60$ the error is almost negligible (around 0.05% for the real part and 0.004% for the imaginary part). Likewise, Tables 3 and 4, show the results obtained for ω_r and ω_i respectively, using the Chebychev differentiation scheme. Here we find that the results converge to the same ω as the FDS, for all the values of L tested, ($1 \leq L \leq 20$). For $N \geq 60$ the error is again negligible (around 0.05% for the real part and 0.004% for the imaginary part).

Table 1: Real Part of ω , Profile I, 6th Order FDS.

	L						
N	10	15	20	25	30	35	40
20	0.19971	0.19991	0.19990	0.19993	0.19993	0.19991	0.19993
60	0.19995	0.20009	0.20009	0.20009	0.20009	0.20009	0.20009
100	0.19991	0.20008	0.20009	0.20009	0.20009	0.20009	0.20009
200	0.19985	0.20008	0.20009	0.20009	0.20009	0.20009	0.20009
300	0.19984	0.20008	0.20009	0.20009	0.20009	0.20009	0.20009
400	0.19983	0.20008	0.20009	0.20009	0.20009	0.20009	0.20009

Table 5 shows a comparison between the different critical values found by Morris [6], Lessen and Singh [3] and that found with our code for the $m = 1$

Table 2: Imaginary Part of ω , Profile I, 6th Order FDS.

	L						
N	10	15	20	25	30	35	40
20	-0.00005	-0.00011	-0.00008	-0.00011	-0.00008	-0.00011	-0.00013
60	-0.00006	-0.00003	-0.00004	-0.00004	-0.00004	-0.00004	-0.00004
100	-0.00006	-0.00003	-0.00004	-0.00004	-0.00004	-0.00004	-0.00004
200	-0.00004	-0.00003	-0.00004	-0.00004	-0.00004	-0.00004	-0.00004
300	-0.00003	-0.00003	-0.00004	-0.00004	-0.00004	-0.00004	-0.00004
400	-0.00002	-0.00002	-0.00004	-0.00004	-0.00004	-0.00004	-0.00004

mode. Since the FDS and the Chebyshev scheme produce the same results for this particular case, the critical value was found using only the FDS. Results for the present investigation fall between those of Morris, and Lessen and Singh

The results obtained by using the far jet profile showed that both the Chebyshev and FDS provide accurate results with a low number of grid points and a wide range of the grid parameter, L . However as is shown in Figure 3.1, this profile is quite smooth and can even be differentiated accurately with a second order differentiation scheme. Since the Reynolds numbers taken into account are low then the low Mach number viscous terms of the code can be considered to have been validated with respect to the previous investigations of Morris and Lessen and Singh.

Table 3: Real Part of ω , Profile I, Chebyshev Differentiation.

	L						
N	1	2	3	4	5	10	20
20	0.20009	0.20009	0.20010	0.20010	0.20007	0.20065	0.20226
60	0.20009	0.20009	0.20009	0.20009	0.20009	0.20009	0.20009
100	0.20009	0.20009	0.20009	0.20009	0.20009	0.20009	0.20009
200	0.20009	0.20009	0.20009	0.20009	0.20009	0.20009	0.20009
300	0.20009	0.20009	0.20009	0.20009	0.20009	0.20009	0.20009
400	0.20009	0.20009	0.20009	0.20009	0.20009	0.20009	0.20009

3.3 Comparison with Inviscid Code

The second validation case tests the inviscid and compressible terms of the equations. First the inviscid code is run for different values of m , α and different z - locations. Then the viscous compressible code developed presently is run for these same parameters and once again the convergence of each differentiation scheme and accuracy of the results is determined. For all the cases the runs are made for a $M = 0.9$ and $Re = 3 \times 10^6$ for which we assume the viscous terms become negligible.

The first case studied uses $m = 0$, $\alpha_r = 1.9$ and $z = 5$. Tables 6 and 7 show the results obtained by varying the parameters N and L and using the FDS. Tables 8 and 9 show the results obtained by varying the parameters N and L and using the Chebyshev differentiation scheme. Once again the converged results agree for either scheme, however the Chebyshev differentiation only converges for a high number of grid points, ($N \geq 200$), and even then it is varying significantly with the parameter L . The convergence with the FDS also requires a greater number of grid points than what was seen

Table 4: Imaginary Part of ω , Profile I, Chebyshev Differentiation.

	L						
N	1	2	3	4	5	10	20
20	-0.00003	-0.00004	-0.00004	-0.00004	-0.00004	0.00030	0.00441
60	-0.00004	-0.00004	-0.00004	-0.00004	-0.00004	-0.00004	-0.00004
100	-0.00004	-0.00004	-0.00004	-0.00004	-0.00004	-0.00004	-0.00004
200	-0.00004	-0.00004	-0.00004	-0.00004	-0.00004	-0.00004	-0.00004
300	-0.00004	-0.00004	-0.00004	-0.00004	-0.00004	-0.00004	-0.00004
400	-0.00004	-0.00004	-0.00004	-0.00004	-0.00004	-0.00004	-0.00004

for the first validation case ($N \geq 100$ in most cases) but is more consistent for all the values of L tested.

When the $m = 1$ mode is tested for $\alpha_r = 1.9$ and $z = 5$, the convergence of both schemes is improved significantly and hence the following test cases will concentrate on the $m = 0$ mode given that obtaining good results is more difficult for this mode.

When we run cases for different z -locations along the jet such as $z = 1$ with $\alpha_r = 7.5$ and $m = 0$ we find that again the FDS converges for $1 \leq L \leq 4$ with $n \geq 60$ yet with $L \geq 10$ more grid points are needed to have convergence, (around $N = 200$) similarly to the previous example at $z = 5$. However, the Chebyshev scheme dose not converge for any of the values of L tested ($1 \leq L \leq 30$), even though up to $N = 400$ grid points were used. This again suggests that the Chebyshev grid parameter is more sensitive to the profile shape than the FDS. Similarly when the code is run at $z = 10$ convergence only happens when using a high number of grid points ($n \geq 300$) for the

Table 5: Comparison of the critical value for the $m = 1$ mode for Profile I.

Case	$Re_{critical}$	$\alpha_{r-critical}$	$\omega_{r-critical}$
Morris	37.64	0.44	0.1
Lessen and Singh	37.9	0.3989	0.08
6th Order FDS Code	37.8	0.417	0.09

FDS and does not happen for the Chebyshev scheme. All this suggests that the grid parameter becomes more and more important when using Profile II and that it should be adjusted depending on the z -location.

Tables 10 and 11 show the converged results obtained for the different differentiation schemes. Once converged, both schemes produce similar results with a negligible error, however using more than 200 grid points can be very time consuming and an even greater number of grid points is necessary when we want to guarantee convergence with the Chebyshev scheme.

Table 6: Real Part of ω . With $m = 0$, and $\alpha_r = 1.9$ for Profile II at $z = 5$. Using the 6th order FDS.

	L					
N	1	3	5	10	20	30
60	1.30514	1.29341	1.29342	1.29342	1.29290	1.29046
100	1.30573	1.29341	1.29342	1.29342	1.29341	1.29331
200	1.30633	1.29342	1.29342	1.29342	1.29342	1.29342
300	1.30640	1.29342	1.29342	1.29342	1.29342	1.29342
400	1.30584	1.29342	1.29342	1.29342	1.29342	1.29342

Table 7: Imaginary Part of ω . With $m = 0$, and $\alpha_r = 1.9$ for Profile II at $z = 5$. Using the 6th order FDS.

	L					
N	1	3	5	10	20	30
60	0.16636	0.16040	0.16040	0.16040	0.16054	0.15650
100	0.16621	0.16040	0.16040	0.16040	0.16040	0.16048
200	0.16462	0.16041	0.16040	0.16040	0.16040	0.16040
300	0.16194	0.16041	0.16040	0.16040	0.16040	0.16040
400	0.15870	0.16041	0.16040	0.16040	0.16040	0.16040

Table 8: Real Part of ω . With $m = 0$, and $\alpha_r = 1.9$ for Profile II at $z = 5$. Using the Chebyshev Differentiation Scheme.

	L					
N	1	3	5	10	20	30
60	1.28841	1.30870	1.32146	1.33068	1.27488	1.26223
100	1.29337	1.29227	1.29101	1.27824	1.26639	1.30293
200	1.29342	1.29341	1.29336	1.29387	1.29568	1.29094
300	1.29342	1.29342	1.29342	1.29340	1.29350	1.29238
400	1.29342	1.29342	1.29342	1.29342	1.29339	1.29326

Table 9: Imaginary Part of ω . With $m = 0$, and $\alpha_r = 1.9$ for Profile II at $z = 5$. Using the Chebyshev Differentiation Scheme.

	L					
N	1	3	5	10	20	30
60	0.16033	0.15659	0.15188	0.18732	0.20219	0.15444
100	0.16066	0.16176	0.16408	0.15165	0.17624	0.20031
200	0.16040	0.16040	0.16040	0.16076	0.15742	0.16683
300	0.16040	0.16040	0.16040	0.16039	0.16072	0.16090
400	0.16040	0.16040	0.16040	0.16040	0.16039	0.16035

Table 10: Results obtained with the 6th Order FDS and comparison with the inviscid code.

m	z	α_r	ω_r	ω_i	%error ω_r	%error ω_i
0	1	7.5	4.15802	1.06061	0.0006	0.0147
0	5	1.9	1.29342	0.16040	0.0012	0.0119
1	5	1.9	1.02530	0.28658	0.0004	0.0058

Table 11: Results obtained with the Chebyshev Differentiation Scheme and comparison with the inviscid code.

m	z	α_r	ω_r	ω_i	%error ω_r	%error ω_i
0	1	7.5	4.15800	1.06059	0.0002	0.0167
0	5	1.9	1.29342	0.16040	0.0012	0.0119
1	5	1.9	1.02530	0.28658	0.0005	0.0063

4 Results

Our aim was to produce a code that can correctly predict the behaviour of the perturbations in a jet flow so that with them we can obtain some insight into the origin of jet noise. For this reason we will be attempting to reproduce the experimental data taken by Stromberg, McLaughlin and Troutt [7]. We use Profile II at different z -locations, and the properties of the flow are taken as: $Re = 3600$, $M = 0.9$ and $Pr = 0.72$. Given the results detailed in the previous section, the sixth order differentiation scheme is used so that we can obtain data at different z -locations without changing the grid parameters, which are: $L = 30$ and $C = 5.0$. The first step is to test the convergence of results for these parameters, this is done for three different z -locations, $z = 0$ with $\alpha_r = 10$, $z = 5$ with $\alpha_r = 2$ and $z = 10$ with $\alpha_r = 0.5$.

Clearly from Tables 12, 13 and 14, the results are converging at all z -locations and modes (0, 1 and 2) such that the parameters chosen can be used throughout the rest of the report. Only at $z = 10$ and $m = 2$ we require up to 200 grid points for the values to converge. The convergence is better than for the inviscid validation case because the Reynolds number is smaller by a factor of 10^3 . All the results from now on will be obtained using a grid with $N = 200$ points in order to guarantee that the results are converged.

The first results obtained are the temporal and spatial growth rate curves at different z -locations shown in Figure 4.1 for the $m = 0$ mode and Figure 4.2 for the $m = 1$ mode. They show that the instabilities are stronger at z -locations close to the origin and they decay as we move in the streamwise direction. The values of α_r and ω_r where the instabilities are a maximum depend greatly on the z -location. At $z = 3$ the temporal disturbance becomes stable at around $\alpha_r = 7$ whereas the spatial disturbance becomes stable for $\omega_r = 3.75$. In both temporal and spatial analysis, the code has trouble following the curves into the stable region because it picks up other stable modes. For the spatial analysis additional problems may arise when nearing stable region because the secant method has trouble converging.

Figure 4.3, shows the temporal and spatial curves at $z = 3$ for each of the different modes. For the temporal case the $m = 1$ mode is slightly more unstable at its maximum than the $m = 0$ mode. However, for the spatial case both modes are practically equally unstable although the maximum occurs

Table 12: Convergence of $z = 0$ with 6th order FDS and Profile II.

N	ω_r			ω_i		
	$m = 0$	$m = 1$	$m = 2$	$m = 0$	$m = 1$	$m = 2$
20	6.29215	6.29112	6.34775	-0.06199	-0.06192	-0.06487
60	5.43593	5.39039	5.31758	1.39653	1.38468	1.31817
100	5.42953	5.40007	5.32802	1.59694	1.58655	1.53827
200	5.42894	5.39938	5.32722	1.59348	1.58298	1.53367
300	5.42894	5.39937	5.32721	1.59351	1.58301	1.53370
400	5.42894	5.39937	5.32721	1.59351	1.58301	1.53370

at a different value of ω_r .

In order to have a better measure of the amplification of these disturbances we use the n -factor, defined in the e^n method as:

$$n = - \int_{z_0}^z \alpha_i(z) dz \quad (4.1)$$

This is a measure of the amplitude of the disturbance and is computed from the eigenvalues obtained in the spatial analysis. It allows us to find the location of the greatest amplification and also the value of ω_r for which this happens. Figure 4.4 shows these results for the three different modes. The $m = 2$ mode has a significantly smaller amplitude than the $m = 0$ and 1 modes, yet the pattern is similar for all. The most unstable z -locations are around $z = 3 - 5$ and the value of ω_r where the amplitude is highest at these z -locations varies between $\omega_r = 2.5 - 3.0$. Near the jet exit, the higher values of the frequency, $\omega_r = 4.0 - 5.5$, are most unstable. Further downstream it is the mid-range values that are most unstable; even further downstream the frequencies between, $\omega_r = 1.5 - 2.5$ produce more unstable disturbances.

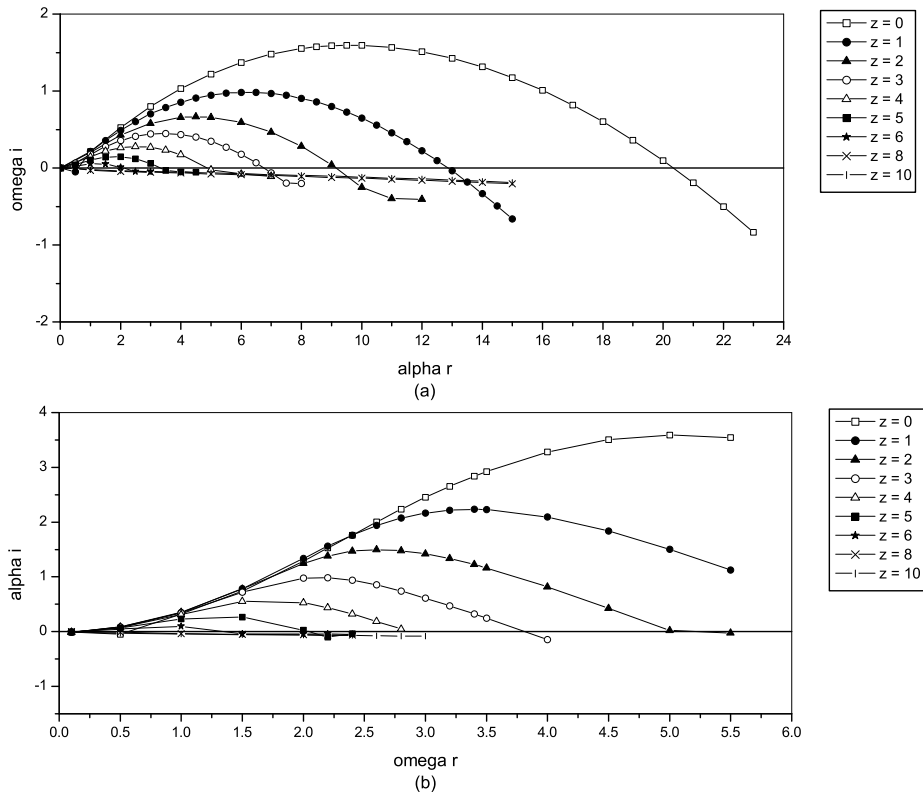


Figure 4.1: (a) Temporal analysis at different z -locations for the $m = 0$ mode. (b) Spatial analysis at different z -locations for the $m = 0$ mode.

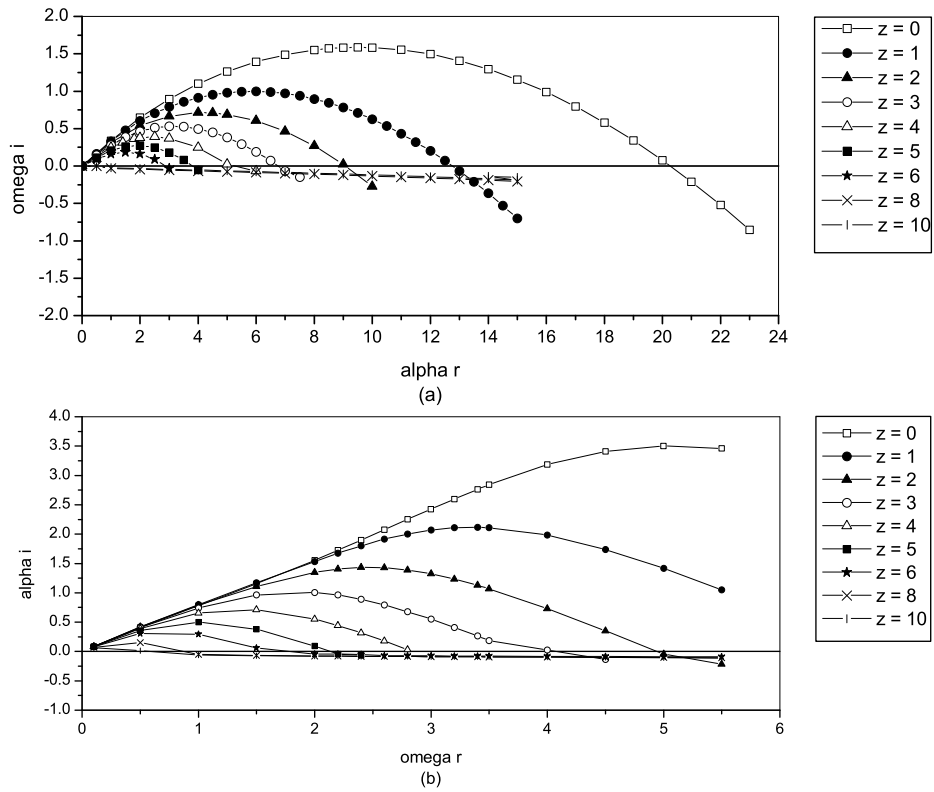


Figure 4.2: (a) Temporal analysis at different z -locations for the $m = 1$ mode. (b) Spatial analysis at different z -locations for the $m = 1$ mode.

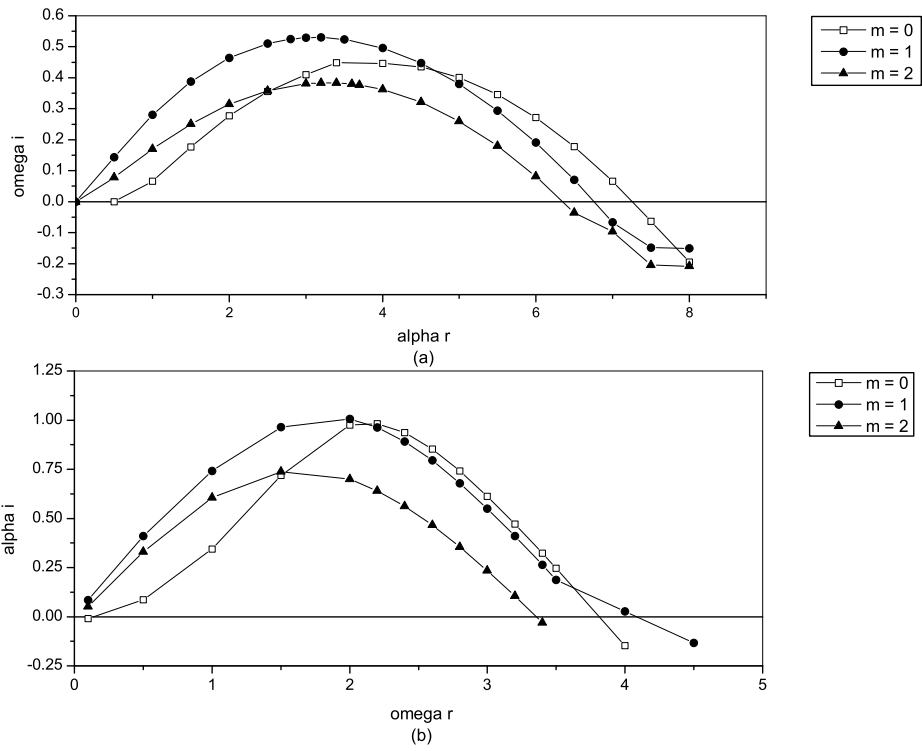


Figure 4.3: (a) Temporal analysis for different modes at the $z = 3$ location. (b) Spatial analysis for different modes at the $z = 3$ location.

Table 13: Convergence of $z = 5$ with 6th order FDS and Profile II.

N	ω_r			ω_i		
	$m = 0$	$m = 1$	$m = 2$	$m = 0$	$m = 1$	$m = 2$
20	1.41511	1.07007	0.92175	0.13610	0.26288	0.10092
60	1.35461	1.08293	0.91841	0.14688	0.27453	0.09105
100	1.35461	1.08293	0.91841	0.14688	0.27453	0.09105
200	1.35461	1.08293	0.91841	0.14688	0.27453	0.09105
300	1.35461	1.08293	0.91841	0.14688	0.27453	0.09105
400	1.35461	1.08293	0.91841	0.14688	0.27453	0.09105

Frequencies, $\omega_r \leq 1.5$ are never strongly amplified.

The highest n -factor, or highest amplitude of the disturbance is found to be at a frequency $\omega_r = 3.0$, with $m = 0$ and $z = 4$. In general the $m = 0$ mode yielded higher amplitudes at each z -location, but the $m = 1$ has a higher amplitude at $z = 5$ whereas the $m = 0$ and 2 modes have it at $z = 4$. In general the frequency that yields the highest amplitudes is between $\omega_r = 2.5 - 3.0$ which corresponds to a Strouhal number, $St = fD/U = \omega/2\pi$, of $St = 0.4 - 0.48$. This matches the results found by Stromberg et al [7], where their peak amplitude was obtained for $St = 0.44$.

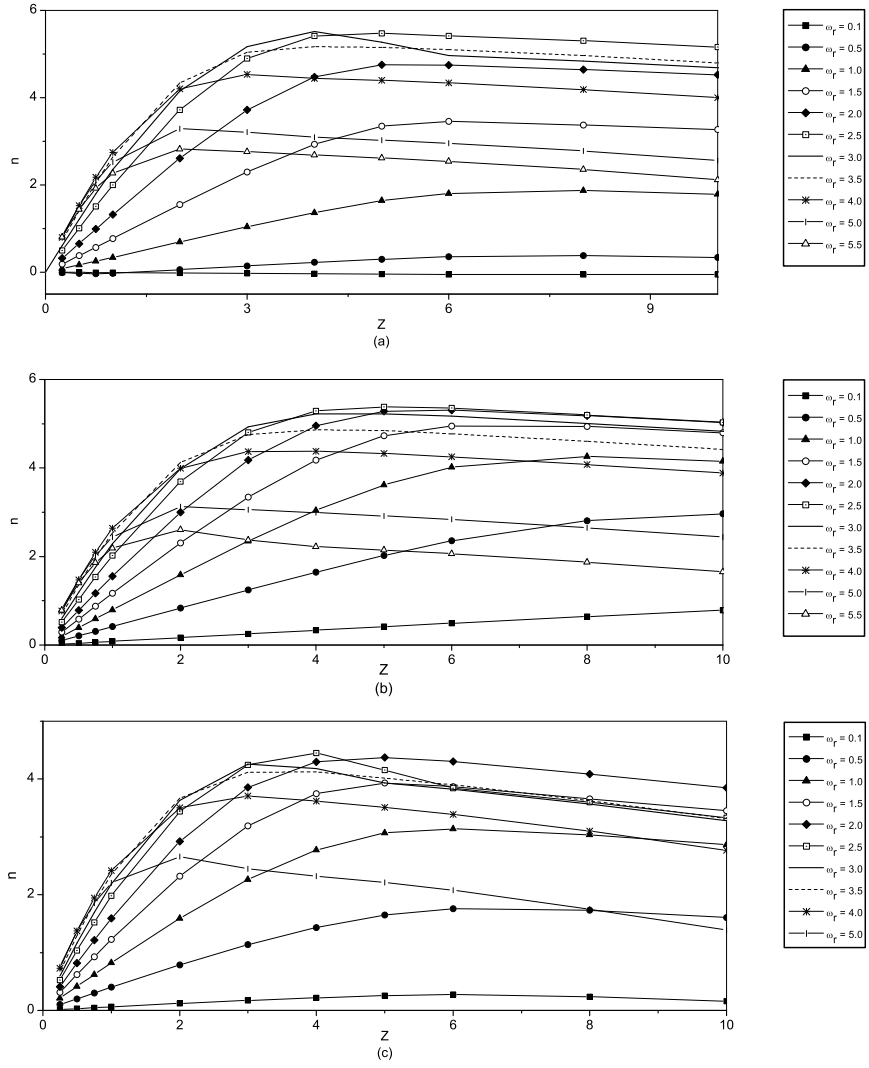


Figure 4.4: Growth factor, n , for different values of ω_r , for: (a) $m = 0$, (b) $m = 1$ and (c) $m = 2$.

Table 14: Convergence of $z = 10$ with 6th order FDS and Profile II.

	ω_r			ω_i		
N	$m = 0$	$m = 1$	$m = 2$	$m = 0$	$m = 1$	$m = 2$
20	0.01154	0.16960	0.07667	-0.00465	0.03305	0.00797
60	0.31987	0.16904	0.00595	-0.01037	0.03324	-0.01395
100	0.31989	0.16904	0.00580	-0.01038	0.03324	-0.02118
200	0.31989	0.16904	0.29149	-0.01038	0.03324	-0.03261
300	0.31989	0.16904	0.29149	-0.01038	0.03324	-0.03261
400	0.31989	0.16904	0.29149	-0.01038	0.03324	-0.03261

5 Conclusions

- A linear stability code to solve the viscous compressible round jet problem has been developed and validated against previous codes. Non-parallel and PSE terms are included in the derivation.
- A sixth order finite difference scheme proved to be better for this application than a Chebyshev differentiation scheme. For the particular Mach and Reynolds numbers used when comparing to experimental data, the grid parameters L and C can remain constant and for most values of z and m . The scheme generally converges for a very low number of grid points.
- When compared to other codes such as Morris [6], Lessen and Singh [3] and Luo and Sandham [5], the errors are all less than (0.05%). When compared to the experimental data the jet Strouhal number is predicted to within 6%.

References

- [1] C. Canuto, M.Y. Hussaini, A. Quarteroni, and T.A. Zang. *Spectral Methods in Fluid Dynamics*. Springer-Verlag, 1988.
- [2] S.K. Lele. Compact finite-difference schemes with spectral-like resolution. *Journal of Computational Physics*, 103, 1992.
- [3] M. Lessen and P.J. Singh. The stability of axisymmetric free shear layers. *Journal of Fluid Mechanics*, 60:433, 1973.
- [4] H. R. Lewis and P.M. Bellan. Physical constraintson the coefficients of fourier exansions in cylindrical coordinates. *Journal of Maths and Physics*, 31:11, Novemeber 1990.
- [5] K.H. Luo and N.D. Sandham. Instability of vortical and acoustic modes in supersonic round jets. *Physics of Fluids*, 9, 2006.
- [6] P.J. Morris. The spatial viscous instability of axisymmetric jets. *Journal of Fluid Mechanics*, 77:511–529, 1976.
- [7] J.L. Stromberg, D.K. McLaughlin, and T.R. Troutt. Flow field and acoustic properties of a mach number 0.9 jet at low reynolds number. *Journal of Sound and Vibration*, 72:159, 1980.

A Vector Definitions in Cylindrical Polar Coordinates

To change from rectangular coordinates to cylindrical polar coordinates we use: $x = r \cos \theta$, $y = r \sin \theta$ and $z = z$. Scale factors and base vectors are defined as follows:

Scale Factors

$$\begin{aligned}
 h_r &= \sqrt{\left(\frac{\partial x}{\partial r}\right)^2 + \left(\frac{\partial y}{\partial r}\right)^2 + \left(\frac{\partial z}{\partial r}\right)^2} = \sqrt{\cos^2 \theta + \sin^2 \theta} = 1 \\
 h_\theta &= \sqrt{\left(\frac{\partial x}{\partial \theta}\right)^2 + \left(\frac{\partial y}{\partial \theta}\right)^2 + \left(\frac{\partial z}{\partial \theta}\right)^2} = \sqrt{(-r \sin \theta)^2 + (r \cos \theta)^2} = r \\
 h_z &= \sqrt{\left(\frac{\partial x}{\partial z}\right)^2 + \left(\frac{\partial y}{\partial z}\right)^2 + \left(\frac{\partial z}{\partial z}\right)^2} = 1
 \end{aligned} \tag{A.1}$$

Base Vectors

$$\begin{aligned}
 \underline{e}_r &= \left(\frac{1}{h_r} \frac{\partial x}{\partial r}, \frac{1}{h_r} \frac{\partial y}{\partial r}, \frac{1}{h_r} \frac{\partial z}{\partial r} \right) = (\cos \theta, \sin \theta, 0) \\
 \underline{e}_\theta &= \left(\frac{1}{h_\theta} \frac{\partial x}{\partial \theta}, \frac{1}{h_\theta} \frac{\partial y}{\partial \theta}, \frac{1}{h_\theta} \frac{\partial z}{\partial \theta} \right) = (-\sin \theta, \cos \theta, 0) \\
 \underline{e}_z &= \left(\frac{1}{h_z} \frac{\partial x}{\partial z}, \frac{1}{h_z} \frac{\partial y}{\partial z}, \frac{1}{h_z} \frac{\partial z}{\partial z} \right) = (0, 0, 1)
 \end{aligned} \tag{A.2}$$

It is important to note that $\frac{\partial \underline{e}_r}{\partial \theta} = \underline{e}_\theta$ and $\frac{\partial \underline{e}_\theta}{\partial \theta} = -\underline{e}_r$.

In order to obtain the Navier-Stokes equation in polar coordinates we need to define the following properties of vectors and scalars.

Gradient of a Scalar, $\nabla\phi$

$$\nabla\phi = \frac{\partial\phi}{\partial r}\underline{e}_r + \frac{1}{r}\frac{\partial\phi}{\partial\theta}\underline{e}_\theta + \frac{\partial\phi}{\partial z}\underline{e}_z \quad (\text{A.3})$$

Gradient of a Vector, $\nabla\underline{V}$

$$\nabla\underline{V} = \begin{pmatrix} \frac{\partial V_r}{\partial r} & \frac{\partial V_\theta}{\partial r} & \frac{\partial V_z}{\partial r} \\ \frac{1}{r}\frac{\partial V_r}{\partial\theta} - \frac{V_\theta}{r} & \frac{1}{r}\frac{\partial V_\theta}{\partial\theta} + \frac{V_r}{r} & \frac{1}{r}\frac{\partial V_z}{\partial\theta} \\ \frac{\partial V_r}{\partial z} & \frac{\partial V_\theta}{\partial z} & \frac{\partial V_z}{\partial z} \end{pmatrix} \quad (\text{A.4})$$

Divergence of a Vector, $\nabla \cdot \underline{V}$

$$\nabla \cdot \underline{V} = \frac{\partial V_r}{\partial r} + \frac{V_r}{r} + \frac{1}{r}\frac{\partial V_\theta}{\partial\theta} + \frac{\partial V_z}{\partial z} \quad (\text{A.5})$$

where $\underline{V} = (V_r, V_\theta, V_z)$

Laplacian of a Scalar, $\nabla^2\phi$

$$\nabla^2\phi = \frac{\partial^2\phi}{\partial r^2} + \frac{1}{r}\frac{\partial\phi}{\partial r} + \frac{1}{r^2}\frac{\partial^2\phi}{\partial\theta^2} + \frac{\partial^2\phi}{\partial z^2} \quad (\text{A.6})$$

Laplacian of a Vector, $\nabla^2\underline{V}$

$$\nabla^2\underline{V} = \begin{pmatrix} \frac{\partial^2 V_r}{\partial r^2} + \frac{1}{r}\frac{\partial V_r}{\partial r} + \frac{1}{r^2}\frac{\partial^2 V_r}{\partial\theta^2} - \frac{V_r}{r^2} - \frac{2}{r^2}\frac{\partial V_\theta}{\partial\theta} + \frac{\partial^2 V_r}{\partial z^2} \\ \frac{\partial^2 V_\theta}{\partial r^2} + \frac{1}{r}\frac{\partial V_\theta}{\partial r} + \frac{2}{r^2}\frac{\partial V_r}{\partial\theta} + \frac{1}{r^2}\frac{\partial^2 V_\theta}{\partial\theta^2} - \frac{V_\theta}{r^2} + \frac{\partial^2 V_\theta}{\partial z^2} \\ \frac{\partial^2 V_z}{\partial r^2} + \frac{1}{r}\frac{\partial V_z}{\partial r} + \frac{1}{r^2}\frac{\partial^2 V_z}{\partial\theta^2} + \frac{\partial^2 V_z}{\partial z^2} \end{pmatrix} \quad (\text{A.7})$$

Curl, $\nabla \times \underline{V}$

$$\nabla \times \underline{V} = \begin{pmatrix} \frac{1}{r} \frac{\partial V_z}{\partial \theta} - \frac{\partial V_\theta}{\partial z} \\ \frac{\partial V_r}{\partial z} - \frac{\partial V_z}{\partial r} \\ \frac{\partial V_\theta}{\partial r} + \frac{V_\theta}{r} - \frac{1}{r} \frac{\partial V_r}{\partial \theta} \end{pmatrix} \quad (\text{A.8})$$

Divergence of a Symmetric Tensor, $\nabla \cdot \underline{s}$

For a symmetric tensor defined as: $\underline{s} = \begin{pmatrix} s_{rr} & s_{r\theta} & s_{rz} \\ s_{\theta r} & s_{\theta\theta} & s_{\theta z} \\ s_{zr} & s_{z\theta} & s_{zz} \end{pmatrix}$.

The divergence is given by:

$$\begin{aligned} (\nabla \cdot \underline{s})_r &= \frac{\partial s_{rr}}{\partial r} + \frac{s_{rr}}{r} + \frac{1}{r} \frac{\partial s_{r\theta}}{\partial \theta} + \frac{\partial s_{rz}}{\partial z} - \frac{s_{\theta\theta}}{r} \\ (\nabla \cdot \underline{s})_\theta &= \frac{\partial s_{r\theta}}{\partial r} + \frac{s_{r\theta}}{r} + \frac{1}{r} \frac{\partial s_{\theta\theta}}{\partial \theta} + \frac{\partial s_{\theta z}}{\partial z} + \frac{s_{\theta r}}{r} \\ (\nabla \cdot \underline{s})_z &= \frac{\partial s_{rz}}{\partial r} + \frac{s_{rz}}{r} + \frac{1}{r} \frac{\partial s_{z\theta}}{\partial \theta} + \frac{\partial s_{zz}}{\partial z} \end{aligned} \quad (\text{A.9})$$

Stress Tensor, \underline{s}

The stress tensor is given by: $\underline{s} = \nabla \underline{u} + \nabla \underline{u}^T - \frac{2}{3} (\nabla \cdot \underline{u}) I$. Here \underline{u} is the velocity vector of the fluid. Therefore the stress tensor of a fluid in polar coordinates can be found, using the previous definitions, to be:

$$(\underline{s})_r = \begin{pmatrix} \frac{4}{3} \frac{\partial V_r}{\partial r} - \frac{2}{3} \left(\frac{V_r}{r} + \frac{1}{r} \frac{\partial V_\theta}{\partial \theta} + \frac{\partial V_z}{\partial z} \right) \\ \frac{\partial V_\theta}{\partial r} + \frac{1}{r} \frac{\partial V_r}{\partial \theta} - \frac{V_\theta}{r} \\ \frac{\partial V_z}{\partial r} + \frac{\partial V_r}{\partial z} \end{pmatrix} \quad (\text{A.10})$$

$$(\underline{s})_\theta = \begin{pmatrix} \frac{\partial V_\theta}{\partial r} + \frac{1}{r} \frac{\partial V_r}{\partial \theta} - \frac{V_\theta}{r} \\ \frac{4}{3} \left(\frac{1}{r} \frac{\partial V_\theta}{\partial \theta} + \frac{V_r}{r} \right) - \frac{2}{3} \left(\frac{\partial V_r}{\partial r} + \frac{\partial V_z}{\partial z} \right) \\ \frac{1}{r} \frac{\partial V_z}{\partial \theta} + \frac{\partial V_\theta}{\partial z} \end{pmatrix} \quad (\text{A.11})$$

$$(\underline{s})_z = \begin{pmatrix} \frac{\partial V_z}{\partial r} + \frac{\partial V_r}{\partial z} \\ \frac{1}{r} \frac{\partial V_z}{\partial \theta} + \frac{\partial V_\theta}{\partial z} \\ \frac{4}{3} \frac{\partial V_z}{\partial z} - \frac{2}{3} \left(\frac{\partial V_r}{\partial r} + \frac{V_r}{r} + \frac{1}{r} \frac{\partial V_\theta}{\partial \theta} \right) \end{pmatrix} \quad (\text{A.12})$$